1 **The paradox of assessing greenhouse gases from soils for nature-**

2 **based solutions**

4 **Authors:**

5 Rodrigo Vargas[1*] and Van Huong Le[1]

7 **Affiliations**

8 [1]Department of Plant and Soil Science, University of Delaware, Newark, DE, USA

11 *Corresponding Author

12 Rodrigo Vargas (rvargas@udel.edu)

20   **Abstract**

21   Quantifying the role of soils in nature-based solutions requires accurate estimates of soil

22   greenhouse gas (GHG) fluxes. Technological advances allow us to measure multiple GHGs

23   simultaneously, and now it is possible to provide complete GHG budgets from soils (i.e.,

24   CO_2, CH_4, and N_2O fluxes). We propose that there is a conflict between the convenience of

25   simultaneously measuring multiple soil GHG fluxes at fixed time intervals (e.g., once or

26   twice per month) and the intrinsic temporal variability and patterns of different GHG fluxes.

27   Information derived from fixed time intervals -commonly done during manual field

28   campaigns- had limitations to reproducing statistical properties, temporal dependence, annual

29   budgets, and associated uncertainty when compared with information derived from

30   continuous measurements (i.e., automated hourly measurements) for all soil GHG fluxes. We

31   present a novel approach (i.e., temporal univariate Latin Hypercube sampling) that can be

32   applied to provide insights and optimize monitoring efforts of GHG fluxes across time. We

33   suggest that multiple GHG fluxes should not be simultaneously measured at a few fixed time

34   intervals (mainly when measurements are limited to once per month), but an optimized

35   sampling approach can be used to reduce bias and uncertainty. These results have

36   implications for assessing GHG fluxes from soils and consequently reduce uncertainty on the

37   role of soils in nature-based solutions.

38

39   **Keywords:** Carbon dioxide, methane, nitrous oxide, representativeness, uncertainty

1. Introduction

Soils are essential for nature-based solutions for their role in climate mitigation potential through implementing different natural pathways (Griscom et al., 2017; Bossio et al., 2020). The climate mitigation potential of soils is dependent on multiple factors such as weather variability (Kim et al., 2012), ecosystem type (Oertel et al., 2016), soil structure (Ball, 2013), management practices (Shakoor et al., 2021), or disturbances (Vargas, 2012), where soils can ultimately act as net sources or sinks of greenhouse gases (GHGs). Therefore, accurate quantification of the magnitudes and patterns of soil GHGs fluxes is needed to understand the potential of soils to mitigate or contribute to global warming across ecosystems and different scenarios.

Most of our understanding of soil GHGs has come from manual measurements performed throughout labor-intensive field campaigns and experiments (Oertel et al., 2016). While most studies around the world have focused on soil CO_2 fluxes (Jian et al., 2020), early examples have reported coupled measurements of soil CO_2, CH_4, and N_2O fluxes across tropical forests (Keller et al., 1986) and savannas (Hao et al., 1988), temperate forests (Bowden et al., 1993), and peatlands (Freeman et al., 1993). These pioneer studies provided an early view of the importance of integrated measurements of multiple soil GHG fluxes to understand the net global warming potential of soils but also demonstrated the technical limitations and challenges associated with these efforts. For example, it is known that manual measurements have the strength of providing good spatial coverage during field surveys but provide limited information about the temporal variability (Yao et al., 2009; Barba et al., 2021).

Technological advances have opened the opportunity to simultaneously measure multiple soil GHG fluxes (i.e., CO_2, CH_4, and N_2O) at unprecedented temporal resolution (e.g., hourly). These efforts have demonstrated differences in diel patterns and pulse events

65 (e.g., rewetting) due to wetting and drying cycles across tropical (Butterbach-Bahl et al.,

66 2004; Werner et al., 2007), subtropical (Rowlings et al., 2012), and temperate (Savage et al.,

67 2014; Petrakis et al., 2017) ecosystems. These approaches provide more accurate information

68 to calculate net GHG budgets and the global warming potential of soils (Capooci et al.,

69 2019). That said, performing automated measurements of multiple GHGs is expensive, and

70 this approach usually has a lower representation of the spatial heterogeneity within

71 ecosystems (Yao et al., 2009; Barba et al., 2021).

72   Ideally, we would like to measure everything, everywhere, and all the time, but this is

73 impossible due to logistical, technological, physical, and economic constraints. Lightweight

74 and low-powered laser-based spectrometers have reduced technical barriers to

75 simultaneously measuring multiple GHGs fluxes from soils. It is now easier and faster to

76 perform discrete manual surveys across time. This opportunity creates a paradox concerning

77 when to measure different GHG fluxes from soils when performing manual measurements.

78 Researchers generally tend to perform simultaneous measurements of multiple GHGs during

79 manual surveys, but this convenience could result in biased information. We propose that

80 there is a conflict between the convenience of measuring multiple GHGs at a few fixed time

81 intervals and the intrinsic temporal variability of magnitudes and patterns of different GHG

82 fluxes.

83   Here, we present a proof-of-concept and test how a subset of measurements derived

84 from a fixed temporal stratification (FTS) for simultaneous measurements (i.e., stratified

85 sampling schedule) or using an optimized sampling (i.e., temporal univariate Latin

86 Hypercube sampling (*tuLHs*)), compared with automated measurements of soil CO_2 (F_ACO_2),

87 CH_4 (F_ACH_4), and N_2O (F_AN_2O) fluxes from a temperate forest (Petrakis et al., 2018; Barba

88 et al., 2021, 2019). The underlying assumption supporting any FTS approach is that a few

89 measurements in time can reproduce the statistical properties and temporal dependencies of

90   soil CO_2, CH_4, and N_2O fluxes because these GHGs respond similarly to biological and

91   physical drivers. The *tuLHs* is a new statistical method for generating subsamples of

92   parameter values (i.e., soil GHG gas fluxes in this case study) to reproduce the probability

93   distribution and the temporal dependence of each original time series of GHG fluxes. We

94   reveal that reporting GHG fluxes using an FTS for simultaneous measurements may result in

95   biased information on temporal patterns and magnitudes. This study shows how a biased

96   sampling schedule could influence our understanding of GHG fluxes and, ultimately, the

97   climate mitigation potential of soils.

98

99   **2. Materials and Methods**

100   *2.1 Study site*

101   The experiment was performed in a temperate forest located at the St Jones Estuarine

102   Reserve (a component of the Delaware National Estuarine Research Reserve [DNERR] in

103   Delaware, USA. The site has a mean annual temperature of 13.3 °C and a mean annual

104   precipitation of 1119 mm. Soils are classified as Othello silt loam with a texture of 40% sand,

105   48% silt, and 12% clay within the first 10 cm (Petrakis et al., 2018). The dominant plant

106   species are bitternut hickory (*Carya cordiformis*), eastern red cedar (*Juniperus virginiana* L.),

107   American holly (*Ilex opaca*), sweet gum (*Liquidambar styraciflua* L.), and black gum (*Nyssa*

108   *sylvatica* (Marshall)). The site has a mean tree density of 678 stems ha^{-1} and a diameter at

109   breast height (DBH) of 25.7±13.9 cm (mean±SD) (Barba et al., 2021).

110

111   *2.2 Automated measurements of soil GHG fluxes*

112   We analyzed data from automated measurements (1hr time intervals) of soil emissions of

113   three GHGs (i.e., CO_2, CH_4, and N_2O) between January and December 2015. This was a

114   typical year with a mean annual temperature of 13.4 °C and an annual precipitation of 1232

115 mm. Continuous measurements of soil GHGs were taken by coupling a closed-path infrared

116 gas analyzer (Li-COR LI-8100 A, Lincoln, Nebraska) and nine dynamic soil chambers (Li-

117 COR 8100–104) controlled by a multiplexer (Li-COR 8100-104) with a cavity ring-down

118 spectrometer (Picarro G2508, Santa Clara, California). A detailed description of the

119 experimental design and measurements protocol is described in previous studies (Petrakis et

120 al., 2018; Barba et al., 2021, 2019). Briefly, for each flux observation, we measured CO_2,

121 CH_4, and N_2O concentrations every second with the Picarro G2508 for 300 seconds and

122 calculated fluxes (at 1 hr time intervals) from the mole dry fraction of each gas (i.e.,

123 corrected for water vapor dilution) using the SoilFluxPro software (v4.0; Li-COR, Lincoln,

124 Nebraska, USA). Fluxes were estimated using linear and exponential fits, and we kept the

125 flux calculation with the highest R^2. We applied quality assurance and quality control

126 protocols using information from all three GHGs as established in previous studies (Petrakis

127 et al., 2018; Barba et al., 2021, 2019; Capooci et al., 2019; Petrakis et al., 2017). Using these

128 time series, we extracted values to represent discrete temporal measurements based on FTS

129 and used the optimization approach described below.

130

131 *2.3 Temporal subsampling of time series*

132 Subsampling of time series was performed using FTS and a temporal optimization following

133 a univariate Latin Hypercube (*tuLHs*) approach. The difference between FTS and temporal

134 optimization is that the first approach is focused on a fixed schedule (e.g., sampling once per

135 month), and the second is focused on reproducing the statistical properties and temporal

136 dependence relationship of the original GHG time series with a subset of measurements. This

137 means optimized subsamples may not be spaced systematically (e.g., every 15 days), and

138 selected dates may vary for each GHG flux due to their specific statistical properties and

139 temporal dependence.

140   FTS represents a traditional schedule for performing manual measurements of GHG

141 fluxes from soils. The FTS is usually performed with manual measurements because they

142 require extensive logistical coordination due to travel time and costs, availability of

143 instrumentation (e.g., gas analyzers), personnel to perform the measurements, and weather

144 conditions. During these scheduled visits, researchers usually collect fluxes from all three

145 GHGs and analyze them systematically to calculate magnitudes and patterns throughout the

146 experiment. Usually, researchers perform manual samples during the early hours of the day

147 (between 9 am and 12 pm) to avoid confounding effects due to large changes in temperature

148 and moisture, as demonstrated by information summarized by the soil respiration global

149 database (Cueva et al., 2017; Jian et al., 2020). Consequently, we selected subsamples from

150 each original GHG time series (derived from automated measurements) using flux

151 measurements from 10 am at fixed intervals of once per month (n=12), twice per month

152 (n=24), or four times per month (n=48) starting on the first week of available data from

153 automated measurements.

154   We applied *tuLHs* as an alternative subsampling approach to obtain an optimized

155 subsample with the same univariate statistical properties and temporal dependence

156 relationship of the original GHG time series. Optimization was performed to select

157 subsamples for each GHG flux using the same number of samples as for FTS: twelve (k=12),

158 twenty-four (k=24), or forty-eight (k=48) measurements throughout the year of available data

159 from automated measurements.

160

161 *2.4 Temporal Univariate Latin Hypercube Sampling (tuLHs)*

162 Let $S = \{(x_1, y_1, z_1), (x_2, y_2, z_2), \ldots, (x_n, y_n, z_n)\}$ be observations of the variables *X, Y,* and *Z* in a

163 time series, where X, Y, and Z are soil GHGs (i.e., CO_2, CH_4, and N_2O). Each measured

164 variable is characterized by the univariate probability distribution function and the temporal

165 dependency function. Once these two functions are known, then the behaviors of the variable

166 can be reproduced (Le et al., 2020; Chilès and Delfiner, 2009; Trangmar et al., 1986; Pyrcz

167 and Deutsch, 2014). The *tuLHs* consists of three steps: (1) modeling the univariate behavior of

168 the variable using the empirical cumulative univariate probability distribution function; (2)

169 modeling the temporal dependence using the empirical variogram function; and (3) optimizing

170 a subsample applying a global optimization method, differential evolution, using the previously

171 obtained variogram function as an objective function.

172 First, to model the univariate behavior of the variables from the observations of S, the

173 empirical univariate cumulative distribution function $F_n^*(x)$ of X is estimated by:

174
$$F_n^*(x) = \frac{1}{n}\sum_{i=1}^{n} I\{x_i \leq x\} \quad (1)$$

175 where *I* represents an indicator function equal to 1 when its argument is true, and 0 otherwise.

176 Similarly, the empirical univariate distribution function of the variables *Y* and *Z* can be derived.

177 Second, to model the temporal dependence of the variables from the observations of *S*, the

178 empirical temporal correlation function (i.e., temporal variogram function) $\gamma^*(t)$ of X is

179 estimated by:

180
$$\gamma^*(t) = \frac{1}{2N(t)}\sum_{i=1}^{N(t)} [X(t_i + t) - X(t_i)]^2 \quad (2)$$

181 where *N(t)* is the number of pairs $X(t_i + t)$ and $X(t_i)$ are separated by a time *t*. The variogram

182 functions of the variables Y and Z are analogous. Third, to optimize the subsample, it is

183 required to choose the "optimal" data points with the selected sample size (i.e., *k*=12, 24, or

184 48; where *k* $<< n)$ that will have the same behavior as the original observations of *S* (i.e., GHG

185 fluxes derived from automated measurements). To achieve this objective, we use differential

186 evolution, a global optimization method (Storn and Price, 1997), using the variogram function

187 as an objective function. The procedure consists of dividing the univariate empirical probability

188   distribution in Eq. (1) into k equiprobable strata, which is equivalent to k ordered data subsets.

189   From each subset, only one value must be chosen to satisfy the condition of a univariate Latin

190   hypercube. The differential evolution method is applied to find the optimal points that

191   minimize the difference between the subsample variogram γ (t) and the data variogram γ * (t)

192   in Eq. (3).

193
$$OF_1 = \sum_{i=1}^{N(t)} [\gamma(t) - \gamma^*(t)]^2 \qquad (3)$$

194   where *OF* is the objective function, and the variograms γ (t) and γ * (t) are calculated using Eq.

195   (2).

196

197   *2.5 Statistical analyses*

198   The t-test was used to compare the means, and the Kolmogorov-Smirnov test was used to

199   compare the probability distribution of measurements derived from each sampling protocol.

200   All tests were done with a 95% confidence level. In addition, their statistical properties, such

201   as mean, median, standard deviation, and first and third quartile, were compared. The

202   differences in the experimental semivariograms were calculated as a comparison measure for

203   the temporal dependence of the samples and the original time series of GHG fluxes. For

204   cumulative sums of GHG flux, their mean is calculated as the most likely value, and their

205   quantile difference between 97.5 and 2.5 is used to quantify the range of uncertainty. All

206   analyzes were performed using the R program (R Code Team, 2013).

207

208   **3. Results**

209   *3.1 Relationships among GHG fluxes from soils*

210   Justification in support of FTS for simultaneous measurements of GHG fluxes would require

211   evidence of strong linear correlations between magnitudes and temporal dependence among

212 soil GHG fluxes. First, we did not find strong linear relationships between any combination

213 of GHG fluxes from soils derived from automated measurements (Fig. S1). Therefore, our

214 data did not support the assumption that the magnitude of one GHG flux was associated with

215 a linear increase or decrease of another GHG flux. Second, semivariogram models

216 demonstrated differences in the temporal dependence for each GHG flux. Automated

217 measurements of soil CO_2 fluxes ($F_A CO_2$) showed a temporal dependence following a

218 Gaussian variogram model, with a nugget of 4, a sill plus nugget of 28, and a correlation

219 range of 80 days (Fig. S2a). Automated measurements of soil CH_4 fluxes ($F_A CH_4$) also

220 showed a temporal dependence but followed a spherical variogram model, with a nugget of

221 7×10^{-8}, a sill plus nugget of 1.5×10^{-7}, and a correlation range of 110 days (Fig. S2b). In

222 contrast, automated measurements of soil N_2O fluxes ($F_A N_2O$) did not show a temporal

223 dependence, where a pure nugget effect was present, and with a correlation range of 0 days

224 (Fig. S2c). Consequently, these GHG fluxes' magnitudes and temporal patterns were different

225 and did not support FTS for simultaneous measurements of GHG from soils.

226

227 *3.2 Optimization of GHG sampling protocols*

228 We applied a *tuLHs* approach to identify subsamples with the same statistical properties and

229 temporal dependence for each of the original GHG time series from automated

230 measurements. Subsamples were identified for twelve ($k=12$), twenty-four ($k=24$), or forty-

231 eight ($k=48$) measurements throughout the year for each GHG time series. Our results show

232 that the optimized measurement dates were different for each GHG flux (Fig. 1), and we

233 provide explicit examples for $k=24$ (Fig. 1) and $k=12, 48$ (Fig. S3, S4).

234   The optimized CO_2 subsamples were well distributed throughout the year for all

235 sampling scenarios (i.e., k from 12 to 48) because $F_A CO_2$ had a strong temporal dependence

236 and a small nugget effect with respect to the sill (Fig. S2a). The optimized CH_4 subsamples

237   were also relatively well distributed throughout the year, especially for scenarios of k=24 and

238   k=48, as F_ACH$_4$ also had a temporal dependence but with a higher nugget effect with respect

239   to the sill (Fig. S2b). Finally, the optimized N$_2$O subsamples were more challenging to

240   define, especially with a small sample size (i.e., k=12; Fig. S3c) because F_AN$_2$O did not have

241   a temporal dependence (Fig. S2c).

242

243   *3.3 Differences in statistical properties and temporal dependency of subsamples*

244   Overall, there were no statistically significant differences between the mean values derived

245   from automated measurements and those from FTS or the *tuLHs* approach (Fig. 2 for k=24;

246   Fig. S5 for k=12; Fig. S6 for k=48; Tables S1 and S2). Although this appears promising, more

247   than a simple comparison of the means is needed to evaluate the information derived from

248   different sampling approaches. In other words, it is possible to have a similar mean value

249   without reproducing the probability distribution nor the temporal dependence of the original

250   time series (i.e., correct answer but for the wrong reasons). Here, we present results based on

251   comparing the means, standard deviation, probability distributions, and semivariograms

252   derived from automated measurements and the different sampling scenarios for all GHG

253   fluxes.

254   The mean of F_ACO$_2$ was 5.9 µmol CO$_2$ m^{-2} s^{-1}, while the mean for FTS 5.5 µmol CO$_2$

255   m^{-2} s^{-1} and 5.9 µmol CO$_2$ m^{-2} s^{-1} for the *tuLHs* approach with k=24 (Fig. 3a-c). These results

256   were comparable with the means derived from FTS (5.4 and 5.4 µmol CO$_2$ m^{-2} s^{-1}) and the

257   *tuLHs* approach (6.2 and 5.9 µmol CO$_2$ m^{-2} s^{-1}) using k=12 and k=48, respectively (Figs. S5,

258   S6; Table S1). The standard deviation of F_ACO$_2$ was 3.9 and 3.2 µmol CO$_2$ m^{-2} s^{-1} for FTS,

259   and 3.9 µmol CO$_2$ m^{-2} s^{-1} for the *tuLHs* approach with k=24 (Figs. 3a-c). These results were

260   comparable with the standard deviations derived from FTS (3.1 and 3.3 µmol CO$_2$ m^{-2} s^{-1}) and

261   the *tuLHs* approach (4.1 and 3.9 µmol CO$_2$ m^{-2} s^{-1}) using k=12 and k=48, respectively (Fig. S5,

262   S6; Table S1). Our results show that the semivariograms of optimized samples using the *tuLHs*

263   approach closely approximate the semivariograms of automated measurements for k=24 (Fig.

264   4a) and k=12 and 48 (Figs. S7a, S8a). These results are consistent with the sums of absolute

265   differences between the semivariograms of the samples and the semivariogram of $F_A CO_2$ with

266   differences of 69.31, 54.39, 49.42 for FTS, and 5.69, 1.99, 1.39 for the *tuLHs* approach for

267   k=12, 24, 48, respectively (Table S2).

268   The mean of $F_A CH_4$ was -0.93 nmol CH_4 m^{-2} s^{-1}, while -0.86 nmol CH_4 m^{-2} s^{-1} for FTS

269   and -0.94 nmol CH_4 m^{-2} s^{-1} for the *tuLHs* approach with k=24 (Fig. 3d-f). These results were

270   also comparable with the means derived from FTS (-0.83 and -0.88 nmol CH_4 m^{-2} s^{-1}) and the

271   *tuLHs* approach (-0.87 and -0.92 nmol CH_4 m^{-2} s^{-1}) using k=12 and 48, respectively (Figs. S5,

272   S6; Table S1). The standard deviation of $F_A CH_4$ was 0.36 and 0.26 nmol CH_4 m^{-2} s^{-1} for FTS

273   and 0.34 nmol CH_4 m^{-2} s^{-1} for the *tuLHs* approach with k=24. These results were comparable

274   with the standard deviations derived from FTS (0.27 and 0.29 nmol CH_4 m^{-2} s^{-1}) and the *tuLHs*

275   approach (0.33 and 0.35 nmol CH_4 m^{-2} s^{-1}) using k=12 and k=48, respectively (Figs. S5, S6;

276   Table S1). The semivariograms of optimized samples using the *tuLHs* approach closely

277   approximate the semivariogram of automated measurements for k=24 (Fig. 4b) and k=12 and

278   48 (Figs. S7b, S8b). Consequently, the sums of absolute differences between the

279   semivariograms of the samples and the semivariogram of $F_A CH_4$ were 0.63, 0.48,0.49 for FTS,

280   and 0.06, 0.04, 0.02 for the *tuLHs* approach with k=12, 24, 48, respectively (Table S2).

281   Finally, the mean of $F_A N_2 O$ was 0.45 and 0.61 nmol $N_2 O$ m^{-2} s^{-1} for FTS, and 0.51 nmol

282   $N_2 O$ m^{-2} s^{-1} for the *tuLHs* approach with k=24 (Fig. 3g-i). These results were also comparable

283   with the means derived from FTS (0.59 and 0.25 nmol $N_2 O$ m^{-2} s^{-1}) and the *tuLHs* approach

284   (0.58 and 0.49 nmol $N_2 O$ m^{-2} s^{-1}) using k=12 and 48, respectively (Figs. S5, S6; Table S1). The

285   standard deviation of $F_A N_2 O$ was 1.62 and 1.97 nmol $N_2 O$ m^{-2} s^{-1} for FTS, and 1.54 nmol $N_2 O$

286   m^{-2} s^{-1} for the *tuLHs* approach with k=24. These results were comparable with the standard

287   deviations derived from FTS (1.38 and 0.91 nmol N_2O m^{-2} s^{-1}) and the *tuLHs* approach (1.58

288   and 1.54 nmol N_2O m^{-2} s^{-1}) using $k=12$ and $k=48$, respectively (Figs. S5, S6; Table S1). Our

289   results show no temporal dependence for N_2O fluxes, but the semivariograms of optimized

290   samples using the *tuLHs* approach closely approximate the semivariogram of automated

291   measurements for $k=24$ (Fig. 4c) and $k=12$ and 48 (Figs. S7c, S8c). Consistently, the sum of

292   absolute differences between the semivariograms of the samples and the semivariogram of

293      $F_A N_2O$ were 10.01, 12.25, 16.75 for FTS, and 0.82, 1.13, 3.57 for the *tuLHs* approach with

294      $k=12$, 24, 48, respectively (Table S2).

295   These results show that the *tuLHs* approach reproduced the probability distribution and

296   the temporal dependence of the time series derived from automated measurements with more

297   precision than FTS for all GHGs. In the next section, we explore the implications of these

298   differences for calculating cumulative GHG fluxes.

299

300   *3.4 Calculation of cumulative GHG fluxes*

301   We calculated the cumulative flux for all GHGs using available information from automated

302   measurements (Fig. 2; Table S3). The cumulative sum for available measurements of $F_A CO_2$

303   was 5758.5 g CO_2 m^{-2} [893.9, 13860.8; 95% CI]; for $F_A CH_4$ was -0.47 g CH_4 m^{-2} [-0.81, -

304   0.19; 95% CI]; and 0.63 g N_2O m^{-2} [-0.75, 5.19; 95% CI] for $F_A N_2O$.

305   We used the mean for each GHG flux derived from the *tuLHs* approach or the FTS to

306   calculate the cumulative sum (Table S3). We found that the FTS underestimated the

307   cumulative flux (-8.4, -6.2, -7.1%) and the uncertainty (-32.6, -21.6, -19.3%) of $F_A CO_2$ for

308      $k=12$, 24, 48, respectively (Fig. 5a). In contrast, the *tuLHs* approach slightly overestimated

309   the cumulative flux (6.5, 1.1, 0.1%) and slightly underestimated the uncertainty (-9.1, -4.4, -

310   3.7%) for $k=12$, 24, 48, respectively (Fig. 5a).

311    The FTS underestimated the cumulative flux (-9.1, -6.1, -3.1%) and the uncertainty (-

312  31.8, -27.3, -15.9%) of $F_A CH_4$ for k=12, 24, 48, respectively (Fig. 5b). In contrast, the *tuLHs*

313  approach underestimated the cumulative flux (-6.1%) only for k=12, but slightly

314  underestimated the uncertainty (-15.9, -6.8, -4.5%) for k=12, 24, 48, respectively (Fig. 5b).

315    The FTS substantially underestimated the cumulative flux (-168, -170, -173%) of

316  $F_A N_2 O$ for k=12, 24, 48, respectively. Uncertainty was overestimated for k=12 and 24 (3.6

317  and 26%) and underestimated for k=48 (-31%; Fig. 5c). In contrast, the *tuLHs* approach

318  overestimated less the cumulative flux (29.5, 13.4, 9.1%) for k=12, 24, 48, respectively (Fig.

319  5c). This approach underestimated the uncertainty for k=12 (-11.2%) and k=24 (-13.8%) but

320  overestimated the uncertainty by 2.9% for k=48 (Fig. 5c). These results show that the *tuLHs*

321  approach consistently provided closer estimates for cumulative sums and uncertainty ranges

322  than an FTS for all GHG fluxes.

323

324  **4. Discussion**

325  Applied challenges, such as quantifying the role of soils in nature-based solutions, require

326  accurate estimates of GHG fluxes. To do this, two fundamental problems exist for designing

327  environmental monitoring protocols: where and when to measure? Ultimately a monitoring

328  protocol aims to quantify the attributes of an ecosystem so that it can be compared in time

329  within that ecosystem or with other ecosystems. Because we cannot measure everything,

330  everywhere, and all the time, we can argue that any monitoring protocol has assumptions

331  based on physical, economic, social, and practical reasons to address a specific scientific

332  question. These assumptions for designing monitoring protocols could result in misleading,

333  biased, or wrong conclusions, and therefore is critical to assess the consequences of different

334  monitoring efforts. As Hutchinson described in "The Concept of Pattern in Ecology," we do

335   not always know if a given pattern is extraordinary or a simple expression of something

336   which we may learn to expect all the time (Hutchinson, 1953).

337   Automated measurements have revolutionized our understanding of the temporal

338   patterns and magnitudes of soil GHG fluxes (Savage et al., 2014; Bond-Lamberty et al.,

339   2020; Tang et al., 2006; Capooci and Vargas, 2022b). These measurements have limitations

340   in representing spatial variability and have higher equipment costs that limit their broad

341   applicability across study sites (Vargas et al., 2011). Consequently, discrete manual

342   measurements are a common approach to simultaneously measure multiple GHG fluxes and

343   report patterns, budgets, and information to parameterize empirical and process-based models

344   (Phillips et al., 2017; Wang and Chen, 2012). In this study, we argue that the convenience of

345   simultaneously measuring multiple GHGs using FTS may result in biased estimates.

346   Therefore, optimization of sampling protocols is needed to provide insights to improve

347   measurement protocols when there is a limited number of measurements in time (i.e., k=12,

348   24, 48).

349   We show that the magnitude of one GHG flux is not associated with a linear increase

350   or decrease of another GHG flux, and the temporal dependencies of each GHG flux are

351   different (Fig. S1). Therefore, it is not possible to infer the dynamics of one GHG flux based

352   solely on information from another under the assumption that they share similar (or

353   autocorrelated) biophysical drivers. These results imply that the magnitudes and temporal

354   patterns of GHGs are different and therefore do not support an FTS approach for

355   simultaneous measurements of GHG fluxes from soils.

356   Multiple studies have shown that the relevance of different biophysical drivers (e.g.,

357   temperature, moisture, light) is different for soil CO_2, CH_4, or N_2O fluxes (Luo et al., 2013;

358   Tang et al., 2006; Ojanen et al., 2010). Our results show that soil CO_2 fluxes have a strong

359   temporal dependence (Fig. S2a), likely due to the strong relationship between these fluxes

360 and soil temperature in this and other temperate mesic ecosystems (Hill et al., 2021; Bahn et

361 al., 2010; Barba et al., 2019). The temporal dependence decreased for soil CH_4 fluxes (Fig.

362 S2b), where there is less evidence for such a strong correlation with soil temperature in this

363 and other temperate mesic ecosystems (Bowden et al., 1998; Castro et al., 1995; Warner et

364 al., 2019; Barba et al., 2019). It has been reported that multiple variables and complex

365 relationships are usually needed to explain the variability of soil CH_4 fluxes in forest soils, as

366 there is a delicate balance between methanogenesis and methanotrophy (Luo et al., 2013;

367 Castro et al., 1994; Murguia-Flores et al., 2018). In contrast, soil N_2O fluxes had no temporal

368 dependence (Fig. S2c), showing decoupling from the observed patterns of soil CO_2 and CH_4

369 fluxes (Wu et al., 2010), likely as a result of independent biophysical drivers regulating soil

370 N_2O fluxes (Luo et al., 2013; Bowden et al., 1993; Ullah and Moore, 2011).

371   To address the limitations of an FTS protocol, we propose a novel optimization

372 approach (i.e., *tuLHs*) to reproduce the probability distribution and the temporal dependence

373 of each original time series of GHG fluxes. Traditional methods usually optimize subsamples

374 by either individually focusing on reproducing the probability distribution of the original

375 information (Huntington and Lyrintzis, 1998) or reproducing the temporal dependence of the

376 original information (Gunawardana et al., 2011). The *tuLHs* is a simple approach that uses

377 the univariate probability distribution function and the temporal correlation function (i.e.,

378 variogram) as objective functions for each GHG flux. Our results show that optimized

379 subsamples do not coincide in time for the three GHGs, suggesting that information should

380 be collected based on each GHG flux's specific statistical and temporal characteristics (Fig.

381 1). This study provides proof-of-concept for the application of the *tuLHs*. It demonstrates

382 how an optimization approach provides insights to design monitoring protocols and improve

383 soil GHG flux estimates.

384   The more temporal data we can collect, the better, but in many cases, measurement

385   protocols are limited to a few measurements per year (i.e., $k=12$ to 48). Our results

386   demonstrate that for a small sample size (i.e., $k=12$), the optimized measurements for soil

387   CO_2 fluxes are consistently spread across the year, and for soil CH_4 fluxes are centered

388   within the growing season because of their strong temporal dependence. For the case of soil

389   N_2O fluxes, the variogram shows a constant temporal variability, meaning there is no

390   temporal dependence. Therefore, the optimized measurements are concentrated within the

391   fall season due to their distribution probability (Fig. 1a). Our optimization approach shows

392   how measurements can be distributed across time as more samples are available (i.e., $k=24$ to

393   48; Fig. 1b-c) and demonstrates that optimization is critical when a limited number of

394   measurements are available. In other words, a few measurements properly distributed across

395   time provide better agreement with information derived from automated measurements. A

396   similar conclusion was proposed for the spatial distribution of environmental observatory

397   networks, where a network of few sites properly distributed (e.g., across a country) improves

398   our understanding of the target variable more than a spatially biased network (Villarreal et

399   al., 2019). Thus, the representativeness assessment of information collected across time and

400   space is needed to evaluate environmental measurements and quantify nature-based solutions

401   accurately.

402   We highlight that this optimization approach should be implemented across different

403   ecosystems as it will result in site-specific recommendations. The *tuLHs* can be applied to

404   any time series length and with any time step (e.g., hours, days), but specific results will be

405   representative of the probability distribution and the temporal dependence of the selected

406   time series. What is essential is to question if a few measurements from an experiment

407   represent the *reality* of the physical world because if limited information is available, then the

408   actual probability distribution and temporal dependence of the phenomena could be an

409   unknown-unknown. In other words, with few measurements, we may not be aware, and we

410   will not be able to know which is the actual probability distribution and temporal dependence

411   of the studied phenomena. To address this challenge, we tested the tuLHs approach with

412   high-temporal frequency information representing the probability distribution of multiple soil

413   GHG fluxes at the daily time-step across a calendar year.

414   In this case study, the year chosen had typical climatological conditions, and we

415   demonstrated that the statistical properties of the different GHG fluxes differ. Consequently,

416   this study questions the application of the FTS approach to measuring multiple GHGs

417   simultaneously with a limited number of sampling dates (mainly once a month). We

418   recognize that longer time series (e.g., multi-year) could provide more robust optimizations

419   that can be applied to monitoring efforts. We recommend co-locating automated

420   measurements with manual survey efforts to adequately capture the temporal and spatial

421   variability of soil GHG fluxes at study sites.

422   There are several implications of biased monitoring protocols for understanding soil

423   GHG fluxes and nature-based solutions. First, temporal patterns and temporal dependency

424   may need to be revisited for studies using an FTS approach. Soil GHG fluxes have complex

425   temporal dynamics that vary from diurnal to seasonal and annual scales (Vargas et al., 2010)

426   that a few measurements following an FTS approach cannot reproduce (Barba et al., 2019;

427   Bréchet et al., 2021). Second, soil GHG fluxes could present hot-moments, which are

428   transient events with disproportionately high values that are often missed with an FTS

429   approach (Vargas et al., 2018; Butterbach-Bahl et al., 2004). Third, cumulative sums and

430   uncertainty ranges are biased or misleading when derived using an FTS approach (Tallec et

431   al., 2019; Lucas-Moffat et al., 2018; Capooci and Vargas, 2022b). Our study demonstrates

432   that an optimized approach consistently provided closer estimates for cumulative sums and

433   uncertainty ranges when compared with automated measurements (Fig. 5). We postulate that

434 representing the variability of soil N_2O fluxes is more sensitive to the FTS approach (>170%

435 and >30% for cumulative sums and uncertainty ranges, respectively) than for soil CH_4 and

436 CO_2 fluxes. Fourth, it is possible that if the information derived from an FTS approach is

437 biased, then functional relationships could also be different from those derived from

438 automated measurements (Capooci and Vargas, 2022a). It has been argued that hypothesis

439 testing and our capability of forecasting responses of soil GHG fluxes to changing climate

440 conditions is also biased with information from the FTS approach (Vicca et al., 2014).

441 Finally, because soils have a central role in nature-based solutions within countries and

442 across the world (Griscom et al., 2017; Bossio et al., 2020), accurate measurements are

443 required to assess management practices, environmental variability, and the contribution of

444 GHGs from soils.

445

446 **Conclusion**

447 We highlight that we only sometimes know if a given pattern is extraordinary or a simple

448 expression of something which we may learn to expect all the time (Hutchinson, 1953).

449 Arguably, there is bias in our understanding of the probability distribution and temporal

450 dependency of soil GHG fluxes across the world because most results are based on a few

451 manual measurements (e.g., once a month) following an FTS approach. Currently, it is

452 unknown how large such bias could be across studies and ecosystems, but because most

453 studies lack high-temporal frequency information, the real probability distribution and

454 temporal dependency of soil GHG fluxes may remain unknown in most study sites. What is

455 essential is to question if the observed patterns, derived from an FTS approach, are enough

456 for improving our understanding of soil processes or are results that we have learned to

457 expect.

458   We postulate that with emergent technologies, there is a convenience of measuring

459   multiple GHGs from soils; however, few measurements collected at fixed time intervals

460   result in biased estimates. We recognize that potential measurement bias depends on each

461   GHG flux's magnitudes and temporal patterns and could be site-specific. Nevertheless,

462   evaluations are needed to quantify potential bias in estimates of GHG budgets and

463   information used for model parameterization and environmental assessments. Furthermore,

464   the underlying assumption that each GHG flux responds similarly to biophysical drivers may

465   need to be tested across multiple ecosystems to quantify how few measurements influence

466   our understanding of magnitudes and temporal patterns of soil GHG fluxes.

467   In this study, we present a proof-of-concept and propose a novel approach (i.e.,

468   temporal univariate Latin Hypercube sampling) that can be applied with site-specific

469   information of different ecosystems to improve monitoring efforts and reduce the bias of

470   GHG flux measurements across time. We highlight that constant biased environmental

471   monitoring may provide confirmatory information, which we have learned to expect, but

472   modifications of monitoring protocols could shed light on new or unexpected patterns. These

473   new patterns are the ones that will test paradigms and push science frontiers.

474

475

476   *Data Availability.* All data used for this analysis is available at:

477   https://doi.org/10.6084/m9.figshare.19536004.v1. The R code used in this study is available

478   at: https://github.com/vargaslab/temporal-univariate-Latin-Hypercube.git

479

480

481   *Author Contributions.* R.V. conceived this study, and V.H.L. designed and performed the

482   primary analysis with input from R.V in all phases. R.V. wrote the manuscript with

483   contributions from V.H.L.

484

485   *Competing Interest Statement.* None

486

487   *Acknowledgments.* The authors thank the Delaware National Estuarine Research Reserve

488   (DNERR) and the St Jones Reserve personnel for their support throughout this study. The

489   authors acknowledge the land on which they realized this study as the traditional home of the

490   Lenni-Lenape tribal nation (Delaware nation). This study was funded by a grant from the

491   National Science Foundation (#1652594) and NASA Carbon Monitoring System

492   (80NSSC21K0964).

     FIGURES
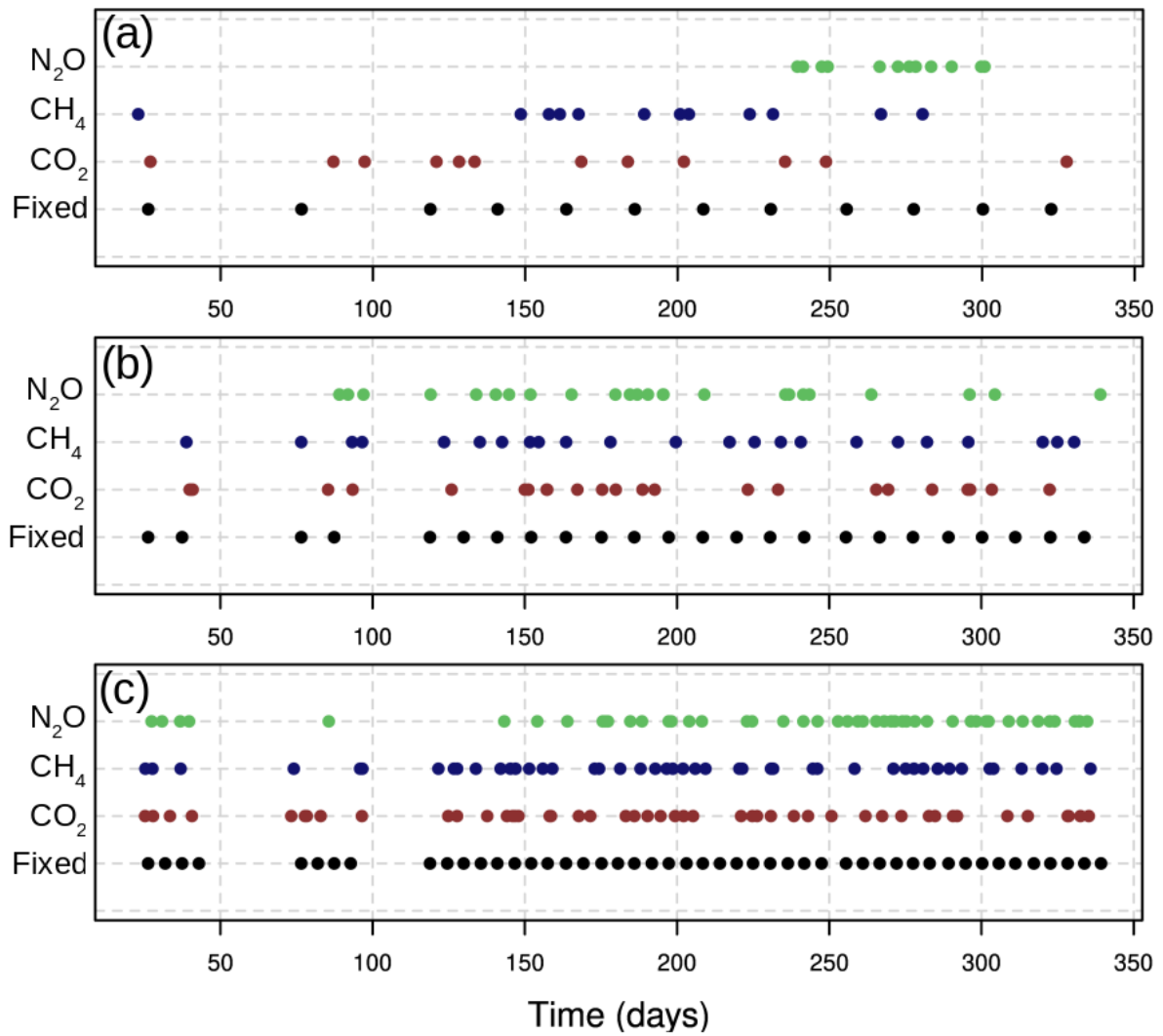
500   **Figure 1.** Temporal distribution of fixed temporal stratification (i.e., stratified manual
501   sampling approach) and optimized sampling using a temporal univariate Latin Hypercube
502   (*tuLHs*) approach for: *k*=12 (a), *k*=24 (b), and *k*=48 (c). Fixed temporal stratification is in
503   black, soil CO_2 fluxes in red, soil CH_4 fluxes in blue, and soil N_2O fluxes in green. Time (x-
504   axis) represents days from January 1 to December 31 of, 2015.

Figure 2. Time series of automated measurements (F_A) of soil greenhouse gas fluxes (black circles) and optimized samples (k=24) using a temporal univariate Latin Hypercube sampling (*tuLHs*) approach for soil CO_2 (a), soil CH_4 (b) and soil N_2O (c) fluxes. The horizontal red line represents the mean, and the horizontal blue line is the median of each greenhouse gas flux derived from automated measurements. The selection of data points for k=12 and 48 are presented for each soil greenhouse gas time series in Figs. S3 and S4, respectively. Time (x-axis) represents days from January 1 to December 31 of, 2015.

517
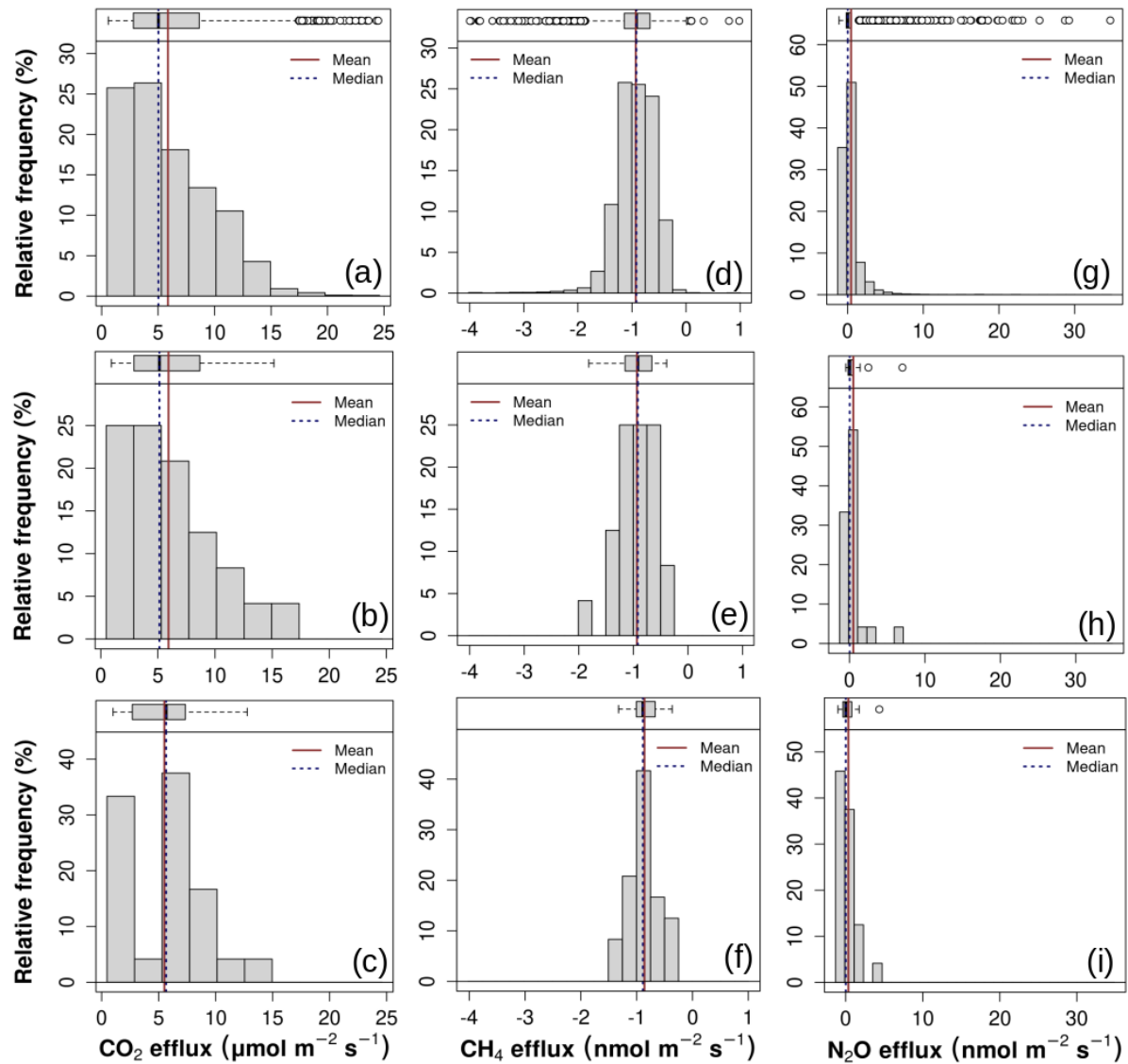
518
519
520
521 **Figure 3**. Histograms for automated measurements of soil CO_2 (F_A CO_2; a), soil CH_4 (F_A
522 CH_4; d), and soil N_2O (F_A N_2O; g). Histograms for optimized samples (k=24) using a
523 temporal univariate Latin Hypercube sampling (*tuLHs*) approach for soil CO_2 (b), soil CH_4
524 (e), and soil N_2O (h) fluxes. Histograms for fixed temporal stratification (i.e., stratified
525 manual sampling schedule) (k=24) for soil CO_2 (c), soil CH_4 (f), and soil N_2O (i) fluxes.
526 Supplementary material includes results for measurements with k=12 (Fig. S5) and k=48
527 (Fig. S6).
528
529
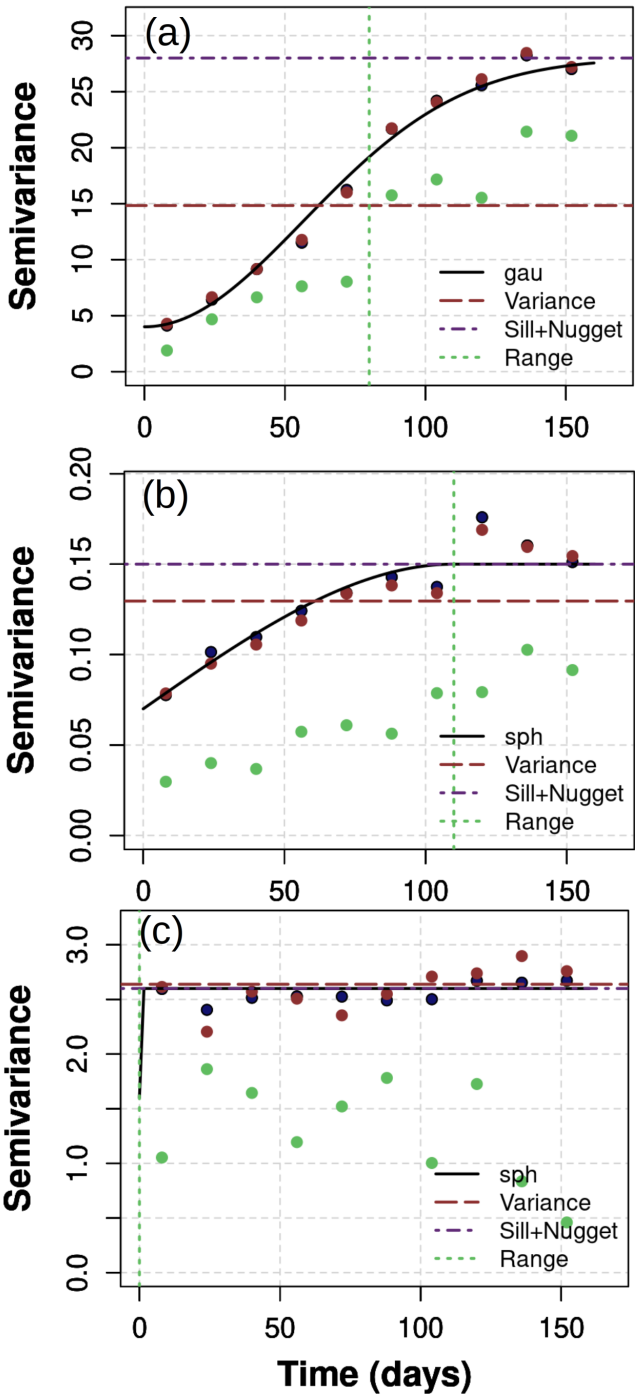
531
532
533
534 **Figure 4**. Comparison of semivariograms between automated measurements (F_A) of soil
535 greenhouse gas fluxes (solid black line) and for optimized samples using a temporal
536 univariate Latin Hypercube sampling (*tuLHs*) approach (red circles) or fixed temporal
537 stratification (green circles) with k=24. Semivarograms are presented for soil CO_2 (a), CH_4
538 (d), and N_2O (c) fluxes. Semivariograms for measurements with k=12 and k=48 are shown in
539 Supplementary Figs. S7 and S8, respectively. Semivariogram fits were gaussian (Gau) or
540 spherical (sph).
541
542
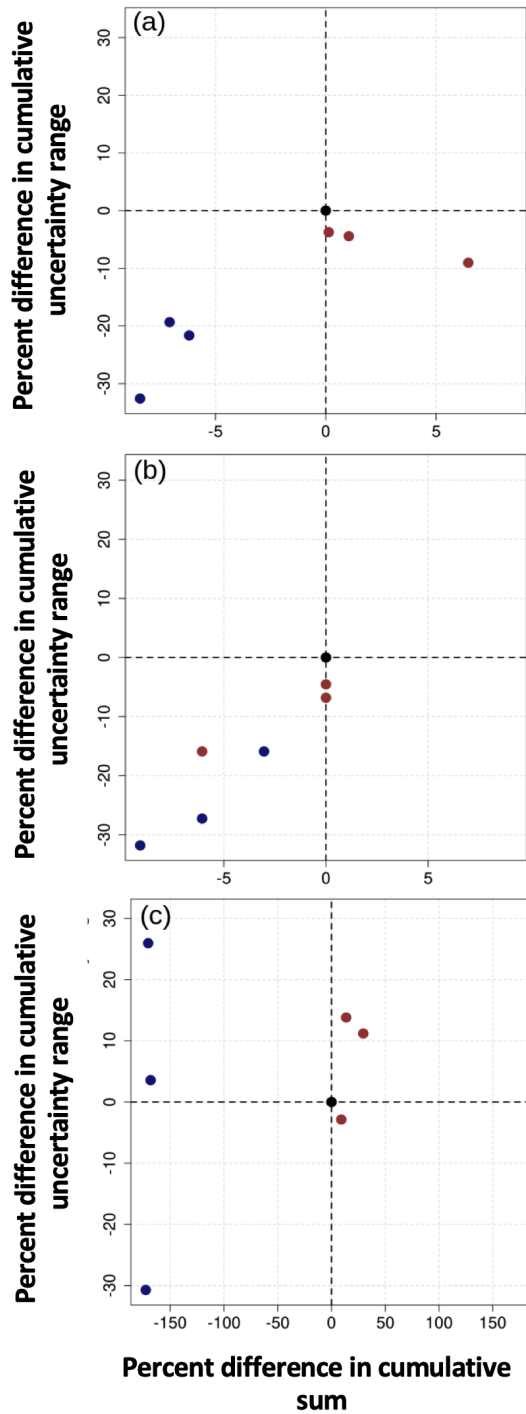
543
544
Figure 5. Comparison of percent differences from cumulative sums and associated
uncertainty (95% CI) between greenhouse gas fluxes derived from automated measurements
(F_A) and using an optimized sampling approach (*tuLHs*) or a fixed temporal stratification.
Differences are represented for soil CO_2 (a), soil CH_4 (b), and soil N_2O (c) fluxes. The black
circle in the center (0,0) of a plot represents the values derived from automated
measurements (F_A). Blue circles represent estimates from fixed temporal stratification, and
red circles represent estimates from an optimized sampling approach (*tuLHs*). Estimates were
calculated based on the 258 available automated measurements (Fig. 2), and numeric
estimates are in Table S3. Note the difference in scale in the x-axis among panels.
554

References

Bahn, M., Reichstein, M., Davidson, E. A., Gruenzweig, J., Jung, M., Carbone, M. S., Epron, D., Misson, L., Nouvellon, Y., Roupsard, O., Savage, K., Trumbore, S. E., Gimeno, C., Curiel Yuste, J., Tang, J., Vargas, R., and Janssens, I. A.: Soil respiration at mean annual temperature predicts annual total across vegetation types and biomes, Biogeosciences, 7, 2147–2157, https://doi.org/10.5194/bg-7-2147-2010, 2010.

Ball, B. C.: Soil structure and greenhouse gas emissions: a synthesis of 20 years of experimentation, Eur. J. Soil Sci., 64, 357–373, https://doi.org/10.1111/ejss.12013, 2013.

Barba, J., Poyatos, R., and Vargas, R.: Automated measurements of greenhouse gases fluxes from tree stems and soils: magnitudes, patterns and drivers, Sci. Rep., 9, 4005, https://doi.org/10.1038/s41598-019-39663-8, 2019.

Barba, J., Poyatos, R., Capooci, M., and Vargas, R.: Spatiotemporal variability and origin of CO_2 and CH_4 tree stem fluxes in an upland forest, Glob. Chang. Biol., 27, 4879–4893, https://doi.org/10.1111/gcb.15783, 2021.

Bond-Lamberty, B., Christianson, D. S., Malhotra, A., Pennington, S. C., Sihi, D., AghaKouchak, A., Anjileli, H., Altaf Arain, M., Armesto, J. J., Ashraf, S., Ataka, M., Baldocchi, D., Andrew Black, T., Buchmann, N., Carbone, M. S., Chang, S., Crill, P., Curtis, P. S., Davidson, E. A., Desai, A. R., Drake, J. E., El-Madany, T. S., Gavazzi, M., Görres, C., Gough, C. M., Goulden, M., Gregg, J., Gutiérrez del Arroyo, O., He, J., Hirano, T., Hopple, A., Hughes, H., Järveoja, J., Jassal, R., Jian, J., Kan, H., Kaye, J., Kominami, Y., Liang, N., Lipson, D., Macdonald, C. A., Maseyk, K., Mathes, K., Mauritz, M., Mayes, M. A., McNulty, S., Miao, G., Migliavacca, M., Miller, S., Miniat, C. F., Nietz, J. G., Nilsson, M. B., Noormets, A., Norouzi, H., O'Connell, C. S., Osborne, B., Oyonarte, C., Pang, Z., Peichl,

578   M., Pendall, E., Perez-Quezada, J. F., Phillips, C. L., Phillips, R. P., Raich, J. W., Renchon,

579   A. A., Ruehr, N. K., Sánchez-Cañete, E. P., Saunders, M., Savage, K. E., Schrumpf, M.,

580   Scott, R. L., Seibt, U., Silver, W. L., Sun, W., Szutu, D., Takagi, K., Takagi, M., Teramoto,

581   M., Tjoelker, M. G., Trumbore, S., Ueyama, M., Vargas, R., Varner, R. K., Verfaillie, J.,

582   Vogel, C., Wang, J., Winston, G., Wood, T. E., Wu, J., Wutzler, T., Zeng, J., Zha, T., Zhang,

583   Q., and Zou, J.: COSORE: A community database for continuous soil respiration and other

584   soil-atmosphere greenhouse gas flux data, Glob. Chang. Biol., 249, 434,

585   https://doi.org/10.1111/gcb.15353, 2020.

586   Bossio, D. A., Cook-Patton, S. C., Ellis, P. W., Fargione, J., Sanderman, J., Smith, P., Wood,

587   S., Zomer, R. J., von Unger, M., Emmer, I. M., and Griscom, B. W.: The role of soil carbon

588   in natural climate solutions, Nature Sustainability, 3, 391–398,

589   https://doi.org/10.1038/s41893-020-0491-z, 2020.

590   Bowden, R. D., Castro, M. S., Melillo, J. M., Steudler, P. A., and Aber, J. D.: Fluxes of

591   greenhouse gases between soils and the atmosphere in a temperate forest following a

592   simulated hurricane blowdown, Biogeochemistry, 21, 61–71, 1993.

593   Bowden, R. D., Newkirk, K. M., and Rullo, G. M.: Carbon dioxide and methane fluxes by a

594   forest soil under laboratory-controlled moisture and temperature conditions, Soil Biol.

595   Biochem., 30, 1591–1597, https://doi.org/10.1016/S0038-0717(97)00228-9, 1998.

596   Bréchet, L. M., Daniel, W., Stahl, C., Burban, B., Goret, J.-Y., Salomón, R. L., and Janssens,

597   I. A.: Simultaneous tree stem and soil greenhouse gas (CO_2 , CH_4 , N_2O) flux

598   measurements: a novel design for continuous monitoring towards improving flux estimates

599   and temporal resolution, New Phytol., 230, 2487–2500, https://doi.org/10.1111/nph.17352,

600   2021.

601   Butterbach-Bahl, K., Kock, M., Willibald, G., Hewett, B., Buhagiar, S., Papen, H., and Kiese,

602   R.: Temporal variations of fluxes of NO, NO2, N2O, CO2, and CH4in a tropical rain forest

603   ecosystem, Global Biogeochem. Cycles, 18, https://doi.org/10.1029/2004gb002243, 2004.

604   Capooci, M. and Vargas, R.: Diel and seasonal patterns of soil CO2 efflux in a temperate

605   tidal marsh, Sci. Total Environ., 802, 149715,

606   https://doi.org/10.1016/j.scitotenv.2021.149715, 2022a.

607   Capooci, M. and Vargas, R.: Trace gas fluxes from tidal salt marsh soils: implications for

608   carbon--sulfur biogeochemistry, Biogeosciences, 19, 4655–4670, https://doi.org/10.5194/bg-

609   19-4655-2022, 2022b.

610   Capooci, M., Barba, J., Seyfferth, A. L., and Vargas, R.: Experimental influence of storm-

611   surge salinity on soil greenhouse gas emissions from a tidal salt marsh, Sci. Total Environ.,

612   686, 1164–1172, https://doi.org/10.1016/j.scitotenv.2019.06.032, 2019.

613   Castro, M. S., Melillo, J. M., Steudler, P. A., and Chapman, J. W.: Soil moisture as a

614   predictor of methane uptake by temperate forest soils, Can. J. For. Res., 24, 1805–1810,

615   https://doi.org/10.1139/x94-233, 1994.

616   Castro, M. S., Steudler, P. A., Melillo, J. M., Aber, J. D., and Bowden, R. D.: Factors

617   controlling atmospheric methane consumption by temperate forest soils, Global Biogeochem.

618   Cycles, 9, 1–10, https://doi.org/10.1029/94gb02651, 1995.

619   Chilès, J.-P. and Delfiner, P.: Geostatistics: Modeling Spatial Uncertainty, John Wiley &

620   Sons, 720 pp., 2009.

621 Cueva, A., Bullock, S. H., López-Reyes, E., and Vargas, R.: Potential bias of daily soil CO2

622 efflux estimates due to sampling time, Sci. Rep., 7, 11925, https://doi.org/ARTN 11925

623 10.1038/s41598-017-11849-y, 2017.

624 Freeman, C., Lock, M. A., and Reynolds, B.: Fluxes of CO2, CH4 and N2O from a Welsh

625 peatland following simulation of water table draw-down: Potential feedback to climatic

626 change, Biogeochemistry, 19, https://doi.org/10.1007/bf00000574, 1993.

627 Griscom, B. W., Adams, J., Ellis, P. W., Houghton, R. A., Lomax, G., Miteva, D. A.,

628 Schlesinger, W. H., Shoch, D., Siikamäki, J. V., Smith, P., Woodbury, P., Zganjar, C.,

629 Blackman, A., Campari, J., Conant, R. T., Delgado, C., Elias, P., Gopalakrishna, T., Hamsik,

630 M. R., Herrero, M., Kiesecker, J., Landis, E., Laestadius, L., Leavitt, S. M., Minnemeyer, S.,

631 Polasky, S., Potapov, P., Putz, F. E., Sanderman, J., Silvius, M., Wollenberg, E., and

632 Fargione, J.: Natural climate solutions, Proc. Natl. Acad. Sci. U. S. A., 114, 11645–11650,

633 https://doi.org/10.1073/pnas.1710465114, 2017.

634 Gunawardana, A., Meek, C., and Xu, P.: A model for temporal dependencies in event

635 streams, Adv. Neural Inf. Process. Syst., 24, 2011.

636 Hao, W. M., Scharffe, D., Crutzen, P. J., and Sanhueza, E.: Production of N2O, CH4, and

637 CO2 from soils in the tropical savanna during the dry season, J. Atmos. Chem., 7, 93–105,

638 https://doi.org/10.1007/bf00048256, 1988.

639 Hill, A. C., Barba, J., Hom, J., and Vargas, R.: Patterns and drivers of multi-annual CO2

640 emissions within a temperate suburban neighborhood, Biogeochemistry, 152, 35–50,

641 https://doi.org/10.1007/s10533-020-00731-1, 2021.

642 Huntington, D. E. and Lyrintzis, C. S.: Improvements to and limitations of Latin hypercube

643 sampling, Probab. Eng. Mech., 13, 245–253, https://doi.org/10.1016/S0266-8920(97)00013-

644 1, 1998.

645 Hutchinson, G. E.: The Concept of Pattern in Ecology, Proceedings of the Academy of

646 Natural Sciences of Philadelphia, 105, 1–12, 1953.

647 Jian, J., Vargas, R., Anderson-Teixeira, K., Stell, E., Herrmann, V., Horn, M., Kholod, N.,

648 Manzon, J., Marchesi, R., Paredes, D., and Bond-Lamberty, B.: A restructured and updated

649 global soil respiration database (SRDB-V5), Data, Algorithms, and Models,

650 https://doi.org/10.5194/essd-2020-136, 2020.

651 Keller, M., Kaplan, W. A., and Wofsy, S. C.: Emissions of N2O, CH4 and CO2 from tropical

652 forest soils, J. Geophys. Res., 91, 11791, https://doi.org/10.1029/jd091id11p11791, 1986.

653 Kim, D. G., Vargas, R., Bond-Lamberty, B., and Turetsky, M. R.: Effects of soil rewetting

654 and thawing on soil gas fluxes: a review of current literature and suggestions for future

655 research, Biogeosciences, 9, 2459–2483, https://doi.org/10.5194/bg-9-2459-2012, 2012.

656 Le, V. H., Díaz-Viera, M. A., Vázquez-Ramírez, D., del Valle-García, R., Erdely, A., and

657 Grana, D.: Bernstein copula-based spatial cosimulation for petrophysical property prediction

658 conditioned to elastic attributes, J. Pet. Sci. Eng., 193, 107382,

659 https://doi.org/10.1016/j.petrol.2020.107382, 2020.

660 Lucas-Moffat, A. M., Huth, V., Augustin, J., Brümmer, C., Herbst, M., and Kutsch, W. L.:

661 Towards pairing plot and field scale measurements in managed ecosystems: Using eddy

662 covariance to cross-validate CO2 fluxes modeled from manual chamber campaigns, Agric.

663 For. Meteorol., 256–257, 362–378, https://doi.org/10.1016/j.agrformet.2018.01.023, 2018.

664   Luo, G. J., Kiese, R., Wolf, B., and Butterbach-Bahl, K.: Effects of soil temperature and

665   moisture on methane uptake and nitrous oxide emissions across three different ecosystem

666   types, Biogeosciences, 10, 3205–3219, https://doi.org/10.5194/bg-10-3205-2013, 2013.

667   Murguia-Flores, F., Arndt, S., Ganesan, A. L., Murray-Tortarolo, G., and Hornibrook, E. R.

668   C.: Soil Methanotrophy Model (MeMo v1.0): a process-based model to quantify global

669   uptake of atmospheric methane by soil, Geosci. Model Dev., 11, 2009–2032,

670   https://doi.org/10.5194/gmd-11-2009-2018, 2018.

671   Oertel, C., Matschullat, J., Zurba, K., Zimmermann, F., and Erasmi, S.: Greenhouse gas

672   emissions from soils—A review, Geochem. Explor. Environ. Analy., 76, 327–352,

673   https://doi.org/10.1016/j.chemer.2016.04.002, 2016.

674   Ojanen, P., Minkkinen, K., Alm, J., and Penttilä, T.: Soil–atmosphere CO_2, CH_4 and N_2O

675   fluxes in boreal forestry-drained peatlands, For. Ecol. Manage., 260, 411–421,

676   https://doi.org/10.1016/j.foreco.2010.04.036, 2010.

677   Petrakis, S., Seyfferth, A., Kan, J., Inamdar, S., and Vargas, R.: Influence of experimental

678   extreme water pulses on greenhouse gas emissions from soils, Biogeochemistry, 133, 147–

679   164, https://doi.org/10.1007/s10533-017-0320-2, 2017.

680   Petrakis, S., Barba, J., Bond-Lamberty, B., and Vargas, R.: Using greenhouse gas fluxes to

681   define soil functional types, Plant Soil, 423, 285–294, https://doi.org/10.1007/s11104-017-

682   3506-4, 2018.

683   Phillips, C. L., Bond-Lamberty, B., Desai, A. R., Lavoie, M., Risk, D., Tang, J. W., Todd-

684   Brown, K., and Vargas, R.: The value of soil respiration measurements for interpreting and

modeling terrestrial carbon cycling, Plant Soil, 413, 1–25, https://doi.org/10.1007/s11104-016-3084-x, 2017.

Pyrcz, M. J. and Deutsch, C. V.: Geostatistical Reservoir Modeling, OUP USA, 433 pp., 2014.

R Code Team: R: A language and environment for statistical computing, 2013.

Rowlings, D. W., Grace, P. R., Kiese, R., and Weier, K. L.: Environmental factors controlling temporal and spatial variability in the soil-atmosphere exchange of CO_2, CH_4 and N_2O from an Australian subtropical rainforest, Glob. Chang. Biol., 18, 726–738, https://doi.org/10.1111/j.1365-2486.2011.02563.x, 2012.

Savage, K., Phillips, R., and Davidson, E.: High temporal frequency measurements of greenhouse gas emissions from soils, Biogeosciences, 11, 2709–2720, https://doi.org/10.5194/bg-11-2709-2014, 2014.

Shakoor, A., Shahbaz, M., Farooq, T. H., Sahar, N. E., Shahzad, S. M., Altaf, M. M., and Ashraf, M.: A global meta-analysis of greenhouse gases emission and crop yield under no-tillage as compared to conventional tillage, Sci. Total Environ., 750, 142299, https://doi.org/10.1016/j.scitotenv.2020.142299, 2021.

Storn, R. and Price, K.: Differential Evolution – A Simple and Efficient Heuristic for global Optimization over Continuous Spaces, J. Global Optimiz., 11, 341–359, https://doi.org/10.1023/A:1008202821328, 1997.

Tallec, T., Brut, A., Joly, L., Dumelié, N., Serça, D., Mordelet, P., Claverie, N., Legain, D., Barrié, J., Decarpenterie, T., Cousin, J., Zawilski, B., Ceschia, E., Guérin, F., and Le Dantec,

706 V.: N2O flux measurements over an irrigated maize crop: A comparison of three methods,

707 Agric. For. Meteorol., 264, 56–72, https://doi.org/10.1016/j.agrformet.2018.09.017, 2019.

708 Tang, X., Liu, S., Zhou, G., Zhang, D., and Zhou, C.: Soil-atmospheric exchange of CO_2 ,

709 CH_4 , and $N_2 O$ in three subtropical forest ecosystems in southern China, Glob. Chang. Biol.,

710 12, 546–560, https://doi.org/10.1111/j.1365-2486.2006.01109.x, 2006.

711 Trangmar, B. B., Yost, R. S., and Uehara, G.: Application of Geostatistics to Spatial Studies

712 of Soil Properties, in: Advances in Agronomy, vol. 38, edited by: Brady, N. C., Academic

713 Press, 45–94, https://doi.org/10.1016/S0065-2113(08)60673-2, 1986.

714 Ullah, S. and Moore, T. R.: Biogeochemical controls on methane, nitrous oxide, and carbon

715 dioxide fluxes from deciduous forest soils in eastern Canada, J. Geophys. Res., 116,

716 https://doi.org/10.1029/2010jg001525, 2011.

717 Vargas, R.: How a hurricane disturbance influences extreme CO_2 fluxes and variance in a

718 tropical forest, Environ. Res. Lett., 2012.

719 Vargas, R., Detto, M., Baldocchi, D. D., and Allen, M. F.: Multiscale analysis of temporal

720 variability of soil CO_2 production as influenced by weather and vegetation, Glob. Chang.

721 Biol., 16, 1589–1605, https://doi.org/10.1111/j.1365-2486.2009.02111.x, 2010.

722 Vargas, R., Carbone, M. S., Reichstein, M., and Baldocchi, D. D.: Frontiers and challenges in

723 soil respiration research: from measurements to model-data integration, Biogeochemistry,

724 102, 1–13, https://doi.org/DOI 10.1007/s10533-010-9462-1, 2011.

725 Vargas, R., Sánchez-Cañete P., E., Serrano-Ortiz, P., Curiel Yuste, J., Domingo, F., López-

726 Ballesteros, A., and Oyonarte, C.: Hot-Moments of Soil CO_2 Efflux in a Water-Limited

727 Grassland, Soil Systems, 2, 47, https://doi.org/10.3390/soilsystems2030047, 2018.

728 Vicca, S., Bahn, M., Estiarte, M., van Loon, E. E., Vargas, R., Alberti, G., Ambus, P., Arain,

729 M. A., Beier, C., Bentley, L. P., Borken, W., Buchmann, N., Collins, S. L., de Dato, G.,

730 Dukes, J. S., Escolar, C., Fay, P., Guidolotti, G., Hanson, P. J., Kahmen, A., Kröel-Dulay, G.,

731 Ladreiter-Knauss, T., Larsen, K. S., Lellei-Kovacs, E., Lebrija-Trejos, E., Maestre, F. T.,

732 Marhan, S., Marshall, M., Meir, P., Miao, Y., Muhr, J., Niklaus, P. A., Ogaya, R., Peñuelas,

733 J., Poll, C., Rustad, L. E., Savage, K., Schindlbacher, A., Schmidt, I. K., Smith, A. R., Sotta,

734 E. D., Suseela, V., Tietema, A., van Gestel, N., van Straaten, O., Wan, S., Weber, U., and

735 Janssens, I. A.: Can current moisture responses predict soil CO2 efflux under altered

736 precipitation regimes? A synthesis of manipulation experiments, Biogeosciences, 11, 2991–

737 3013, https://doi.org/10.5194/bg-11-2991-2014, 2014.

738 Villarreal, S., Guevara, M., Alcaraz-Segura, D., and Vargas, R.: Optimizing an

739 Environmental Observatory Network Design Using Publicly Available Data, J. Geophys.

740 Res. Biogeosci., 124, 1812–1826, https://doi.org/10.1029/2018JG004714, 2019.

741 Wang, G. and Chen, S.: A review on parameterization and uncertainty in modeling

742 greenhouse gas emissions from soil, Geoderma, 170, 206–216,

743 https://doi.org/10.1016/j.geoderma.2011.11.009, 2012.

744 Warner, D. L., Guevara, M., Inamdar, S., and Vargas, R.: Upscaling soil-atmosphere CO2

745 and CH4 fluxes across a topographically complex forested landscape, Agricultural and forest,

746 264, 80–91, https://doi.org/10.1016/j.agrformet.2018.09.020, 2019.

747 Werner, C., Kiese, R., and Butterbach-Bahl, K.: Soil-atmosphere exchange of N2O, CH4,

748 and CO2and controlling environmental factors for tropical rain forest sites in western Kenya,

749 J. Geophys. Res., 112, https://doi.org/10.1029/2006jd007388, 2007.

750   Wu, X., Brüggemann, N., Gasche, R., Shen, Z., Wolf, B., and Butterbach-Bahl, K.:

751   Environmental controls over soil-atmosphere exchange of N2O, NO, and CO2in a temperate

752   Norway spruce forest, Global Biogeochem. Cycles, 24,

753   https://doi.org/10.1029/2009gb003616, 2010.

754   Yao, Z., Zheng, X., Xie, B., Liu, C., Mei, B., Dong, H., Butterbach-Bahl, K., and Zhu, J.:

755   Comparison of manual and automated chambers for field measurements of N2O, CH4, CO2

756   fluxes from cultivated land, Atmos. Environ., 43, 1888–1896,

757   https://doi.org/10.1016/j.atmosenv.2008.12.031, 2009.